The heat-of-mixing effect on ion-induced grain growth

Dale E. Alexander[a] and Gary S. Was
Department of Nuclear Engineering, University of Michigan, Ann Arbor, Michigan 48109

L. E. Rehn
Argonne National Laboratory, 9700 S. Cass Avenue, Argonne, Illinois 60439

(Received 5 November 1990; accepted for publication 18 April 1991)

Irradiation experiments were conducted on multilayer (ML) and coevaporated (CO) thin films in order to examine the role that the heat-of-mixing (ΔH_{mix}) has in ion-induced grain growth. Room-temperature irradiations using 1.7-MeV Xe ions were performed in the High Voltage Electron Microscope at Argonne National Laboratory. The ML films (Pt-Ti, Pt-V, Pt-Ni, Au-Co, and Ni-Al) spanned a large range of calculated ΔH_{mix} values. Comparison of grain growth rates between ML and CO films of a given alloy confirmed a heat-of-mixing effect. With the exception of the Pt-V system, differences in grain growth rates between ML and CO films varied according to the sign of the calculated ΔH_{mix} of the system. Substantial variations in growth rates among CO alloy films experiencing similar displacement damage demonstrated that a purely collisional approach is inadequate for describing ion-induced grain growth. Therefore consideration must also be given to material-specific properties, such as cohesive energy.

I. INTRODUCTION

Ion beams are routinely used to modify the microstructure of thin films and surfaces. Ion irradiation has been observed to cause nearly athermal grain growth in initially fine-grained ($\lesssim$100 Å) polycrystalline thin films. Because grain size controls many important thin-film properties (for example, electromigration characteristics), ion-induced grain growth has been the subject of a number of studies. Investigators have systematically examined the effect of irradiation and material parameters on grain growth in elemental metal[1–12] and semiconductor[3,4] thin films, and in coevaporated metal alloy[10,13] films. In spite of the large number of studies, a comprehensive understanding of the effect of ion irradiation on grain growth is still lacking. Grain growth has also been reported during ion beam mixing experiments in a number of different multilayered alloy films.[14–23] However, unlike elemental and coevaporated alloy films, systematic studies of ion beam mixing induced grain growth, addressing various irradiation and material parameters, have not previously been reported.

Previous work[22] examining the effects of ion beam mixing in the Ni-Al system suggested that the heat-of-mixing, ΔH_{mix}, affected ion-induced grain growth. Multilayer Ni-Al films underwent greater grain growth than coevaporated films of the same composition under identical irradiation conditions.[22] The results indicated that the initial structure of the films (multilayer versus coevaporated) strongly influenced subsequent ion-induced grain growth. One consequence of the multilayer structure was a ΔH_{mix} release induced by ion mixing. This ΔH_{mix} release, absent in the coevaporated films, could have enhanced grain growth rates in the multilayer films.

A goal of the present work is to further investigate the effect of ΔH_{mix} on ion-induced grain growth by examining a variety of multilayer alloys with a broad range of calculated heats-of-mixing, and comparing their growth rate with those of their coevaporated counterparts.

II. BACKGROUND

Systematic irradiation experiments have been conducted to examine the effect of ion mass/energy, dose, dose rate, temperature, and material properties on ion-induced grain growth. In this section, we summarize some of the important results obtained from previous studies.

Grain size in thin films has been consistently observed to be a monotonically increasing function of ion dose. In experiments performed by Wang *et al.*[1,2] grain size in Ni films showed a linear dependence on dose of Ag and Bi ions. More recent studies by Atwater *et al.*,[3,4] Liu *et al.*,[6] and Alexander *et al.*[22] covered a wide variety of ions and targets and showed an exponential dependence of average grain size, L, on ion dose, Φ, of the form $L \propto \Phi^{1/n}$ with the growth exponent, n, varying such that $2 \leqslant n \leqslant 3$. Neither Liu *et al.*[6] nor Atwater *et al.*[3] were able to detect dose rate effects. In these studies, dose rates were varied by an order of magnitude with negligible effect on total grain growth achieved following a fixed dose.

Irradiation is generally observed to induce normal grain growth in which the average grain size increases in a uniform fashion. The uniformity of grain growth combined with the dose dependence of grain size (or time dependence for a constant dose rate) are analogous to grain growth behavior observed in isothermal annealing experiments.[24] The similarity suggests that the same driving force is operative in both. The driving force most typically associated with normal grain growth is the system energy reduction resulting from the reduction in the grain boundary surface area.[24] Secondary (nonuniform) grain growth,

[a]Present address: Argonne National Laboratory, MSD-212, 9700 S. Cass Ave., Argonne, IL 60439.

 0021-8979/91/031252-09$03.00

driven by surface energy anisotropy,[25] is another type of growth sometimes observed to dominate normal grain growth during thermal annealing of thin films. During ion irradiation however, normal grain growth is induced in films despite the fact that the same films exhibit secondary grain growth during annealing in the absence of irradiation.[5,7] It is unclear why irradiation-induced grain growth should be selectively affected by the surface energy reduction driving force and not by surface energy anisotropy.

It should be noted that although these observations support a continuous boundary migration model of ion-induced grain growth, other studies suggest different mechanisms of growth. *In situ* irradiation studies of columnar grained Au films indicate that coalescence is also an important process through which irradiation-induced grain growth can occur.[9] This has led Allen *et al.*[11] to speculate that dislocations have an important role in ion-induced grain growth.

A weak temperature dependence for ion-induced grain growth has been observed, as evidenced by measurements of small activation energies. Atwater *et al.*[3] determined activation energies for ion-induced grain growth in Ge and Si films. They measured activation energies of 0.15 eV for Ge films irradiated in the temperature range of 450–700 °C, and $\leq$0.1 eV for Si films irradiated between 750–850 °C. In a study of Cu films, Liu *et al.*[6] identified two temperature regimes of ion-induced grain growth. Below $-$ 60 °C, grain growth was independent of temperature but above this temperature, ion-induced grain growth displayed a weak temperature dependence with an activation energy of 0.14 eV.

For a given target, heavier ions induce greater grain growth per ion than lighter ions. This behavior is a direct result of the irradiation damage induced by different mass ions. Heavier ions induce more atom displacements because they deposit a greater damage energy, F_D. However, there is uncertainty as to the exact nature of the grain growth rate dependence on F_D. The work of Wang *et al.*[1,2] and Atwater *et al.*[3] indicated a linear dependence of irradiation-induced grain growth rate on F_D, while Liu *et al.*[13] failed to identify the same linear dependence, suggesting instead a dependence on F_D^2. Films of Ni and Pd irradiated with diatomic As_2^+ showed enhanced grain growth when compared with monoatomic irradiation in which the same energy per As atom was maintained.[8] These latter results indicate the importance of deposited damage energy density in ion-induced grain growth.

While irradiation parameters are obviously influential, studies have demonstrated that intrinsic material properties, apart from those associated with irradiation properties (mass and atomic number), are also important. Irradiation of Au and Pt films with Ar ions yielded a grain growth rate in Au that was $\sim$3.5 times greater than in Pt.[5] This occurred despite the similar mass and energy displacement thresholds (E_d) of these elements, which would in turn imply similar collisional effects during irradiation. Parallel annealing studies[5] of these films determined that the activation energy for thermally induced grain growth in Au (0.5 eV) was nearly half that of Pt (0.9 eV). This suggested that the irradiation-induced mobility of grain boundaries is greater in Au than in Pt. Similar behavior was observed in other irradiated elemental and coevaporated alloys. Liu found that a grain boundary mobility related parameter varied with the cohesive energy, ΔH_{coh}, of the material.[13] Greater grain growth was therefore induced in those materials with low cohesive energy. These results were similar to those of Li *et al.*[5] assuming the activation energy for grain growth scales with the cohesive energy.

Grain growth has also been reported during ion beam mixing experiments in a number of different alloy systems. However, unlike elemental and coevaporated alloy films, systematic studies, that address various irradiation and material parameters, of ion beam mixing-induced grain growth, are limited to our previous work.[22] Tsaur *et al.*,[14] in studies of phase formation in ion beam mixed multilayers, observed irradiation-induced growth in various alloys including Ag-Cu (Ref. 16) and Au-Ni.[14,17] Ion beam mixing-induced grain growth was observed in phase formation studies of Ni-rich, Ni-Al multilayers.[15,18] Growth in bilayer mixing experiments in Fe-Al,[19] Ni-Pd,[20] and Bi-Sb (Ref. 21) has also been reported.

We have previously reported a systematic study examining the effect of Xe ion irradiation on grain growth in Ni-Al multilayers and coevaporated thin films.[22] In that work, grain size as a function of ion dose was examined for room-temperature irradiation of Ni-Al multilayer and coevaporated thin films of the same nominal composition. A factor of 2 greater grain size was achieved in the multilayers compared with the coevaporated films irradiated to the same dose of 700-keV Xe ions indicating that the initial structure of the films, multilayered versus coevaporated, influenced ion-induced grain growth.

An enthalpy release associated with the heat-of-mixing, ΔH_{mix}, is a possible mechanism through which the initial structure of the films might have affected ion-induced grain growth. This enthalpy release during irradiation would have occurred in the multilayers but would have been absent in the homogenized coevaporated films. The energy release could have lead to enhanced atomic motion and hence faster grain growth in the multilayers. The heat-of-mixing might also have affected the kinetics of grain growth via a Darken effect,[26] in which atomic diffusion is enhanced across composition gradients. Such an effect has been proposed to explain enhanced ion beam mixing efficiencies observed in systems with large negative heats-of-mixing.[27]

It is clear from this review that a number of parameters impact the phenomenon of ion-induced grain growth. The similarity between the Ni-Al results and previous ion beam mixing studies suggests that a heat-of-mixing effect may also have a role in the observed enhancement in grain growth between multilayer and coevaporated thin films. In order to test this hypothesis, the following study was conducted examining ion-induced grain growth in five different alloys spanning a larger range of calculated ΔH_{mix} values. A heat-of-mixing effect would be expected in

TABLE I. Summary of material and irradiation parameters used in 1.7 MeV Xe ion-induced grain growth studies.

A-B alloy (at. %)	Film type[a]	$\Delta H_{coh(AB)}$[b] (eV)	ΔH_{mix}[c] (eV)	F_D[d] (eV/Å)	Ion range (Å)[e] $R_p \pm \Delta R_p$
Pt-15 Ti	ML	−6.21	−0.52	360	···
Pt-15 Ti	CO	−6.21	none	360	1590±640
Pt-18 V	ML	−6.03	−0.28	360	···
Pt-15 V	CO	−6.04	none	360	1560±630
Ni-21 Al	ML	−4.45	−0.23	225	···
Ni-23 Al	CO	−4.43	none	225	2150±590
Pt-21 Ni	ML	−5.58	−0.03	380	···
Pt-17 Ni	CO	−5.63	none	380	1520±620
Au-20 Co	ML	−3.89	+0.04	340	···
Au-10 Co	CO	−3.83	none	335	1680±690

[a]Film type: ML = multilayers; CO = coevaporated.
[b]Average alloy cohesive energies determined from elemental values (Ref. 28) according to $\Delta H_{coh(AB)} = f_A \Delta H_{coh(A)} + f_B \Delta H_{coh(B)} + \Delta H_{mix}$, where f_A and f_B are the atom fractions of the A and B alloy elements, respectively.
[c]Heat-of-mixing values approximated by values of formation enthalpies for stoichiometric A_5B alloys (Refs. 29–31).
[d]Deposited damage energies calculated using TRIM-90 Monte Carlo simulation (Ref. 32). The quoted F_D is the average over the 400 Å of the film thickness.
[e]Ion ranges and straggling calculated using TRIM-89 Monte Carlo simulation (Ref. 32).

irradiated multilayers but not in the coevaporated films, and thus would manifest itself through differences in grain growth rates between the two film types.

III. EXPERIMENT

Thin (~400 Å) films of coevaporated or multilayered alloy films were prepared by electron beam evaporation in an oilless, cryopumped vacuum system with a pressure of 2×10^{-7} Torr or less during deposition. Deposition rates varied depending on the metal but were usually between 1–10 Å/s. Multilayer films were prepared by sequential evaporation of each alloying element without breaking vacuum. The relative thickness of the individual layers was adjusted to yield the desired overall film composition. For coevaporated films, simultaneous deposition from two separate sources was conducted with the relative deposition rates of the sources controlled to yield the desired film composition.

Since the heat-of-mixing was suspected to influence ion-induced grain growth, the alloys chosen for study spanned a large range of calculated ΔH_{mix} values. Table I summarizes the material and irradiation parameters of the alloys used. With the exception of Ni-Al, all the alloys possessed similar mass ratios and therefore had similar deposited damage energies (F_D) as determined from TRIM-90 calculations.[32] Also shown in Table I are the average alloy cohesive energies, ΔH_{coh}, which were determined from elemental cohesive energy values[28] as indicated in the table.

It is emphasized that the ΔH_{mix} values given in Table I are calculated approximations. The lack of experimental data on ΔH_{mix} in *irradiated* multilayer alloys prompted an approach adopted previously in ion beam mixing studies, in which ΔH_{mix} is approximated by the calculated alloy formation enthalpy, ΔH_{for}, as determined by the model of Miedema and coworkers.[29–31,33] Clearly, such an approximation is not strictly correct since the introduction of irradiation-induced defects (Frenkel pairs, antisite defects, etc.) results in a higher free energy state for the ion beam mixed multilayers than for an equilibrium, homogenized alloy. Hence the magnitude of ΔH_{mix} is actually different than the magnitude of ΔH_{for}. However, in the absence of experimental data, this approach provides a standardized "ruler" by which to determine formation enthalpies and in turn, calculated ΔH_{mix} values for the metal alloys of interest.

Films of *A*-rich *A-B* alloys were made where A = Ni, Pt or Au, and B = Al, Ti, V, Ni, and Co. *A*-rich alloys were chosen to avoid amorphization of the microstructure commonly observed to occur during ion beam mixing of equiatomic and *B*-rich alloy films with large negative heats of mixing.[34] In multilayers, the A layers (A = Ni, Pt, or Au) were typically of the order of 50–60 Å thickness and the B layers (B = Al, Ti, V, Ni, or Co) were typically 10–20 Å thick. The use of thin layers avoided significant ion-induced grain growth within elemental layers prior to mixing. The A elements, being the more inert of the two components in the binary alloy, were deposited on the outer surfaces of the multilayers to minimize oxidation effects. The same was done for the coevaporated films in which thin, approximately 20-Å-thick layers of the inert A element were deposited on both surfaces of the film.

Films were deposited onto Cu TEM grids embedded in an amorphous Crystalbond® substrate on glass microscope slides. After the evaporation, the grids were removed from the glass slides by dissolving the Crystalbond® in acetone, allowing the films to span the holes of the grids. Compositions of the as-evaporated films was determined using x-ray energy dispersive spectroscopy (XEDS) on a JEOL 2000FX TEM.

Electron diffraction was used to examine the films before and during irradiation. Analysis of the coevaporated samples indicated that as-evaporated films existed as single phase solid solutions of element B in the fcc phase of element A. These structures represented non-equilibrium phases in all the alloys except Pt-Ni, in which both elements are completely miscible across the entire phase diagram.[35]

Room-temperature irradiations were conducted in the High Voltage Electron Microscope (HVEM) in the Materials Science Division at Argonne National Laboratory.[36] The HVEM was interfaced with a beamline from a tandem accelerator and *in situ* irradiations were performed using 1.7-MeV Xe ions. As indicated in Table I the average projected range, R_p, minus the straggling, ΔR_p, of the ions was substantially beyond the film thickness and thus avoided significant deposition of Xe in the films. The HVEM was operated at 200 kV, below the threshold for electron irradiation damage in all the elements except Al.

Irradiations were conducted with the ion beam inclined approximately 16° with respect to the film surface normal. Initially, during low dose studies [$(1–3) \times 10^{13}$ cm^{-2}] the dose rate was 1.7×10^{11} cm^{-2} s^{-1}. For doses

$\geq 1\times10^{14}$ cm^{-2} the rate was increased to 1.7×10^{12} cm^{-2} s^{-1}. The lower dose rate was used to control more accurately the ion dose in the low dose regime. The dose rates were also chosen to avoid beam induced heating. The vacuum during irradiation was typically in the 10^{-6} Torr range.

Grain size measurements were obtained from dark field TEM images of microstructures of as-evaporated and irradiated films after various increments of ion dose. Dark field imaging was performed using the (111) fcc, A-phase, reflections. Images were recorded at $50k\times$ magnification and prints were made with a factor of about $2.5\times$ further increase in magnification. Prior to analysis the prints from a number of different samples were randomized in order to avoid biasing results. Grain size measurements were obtained by measuring the largest lateral dimension of highlighted grains in the dark field imaged prints. At least 200 grains were measured per sample. Measurements were facilitated by use of a digitizing tablet interfaced with a PC. Data from the tablet were output as text files to the PC. Using this technique, large amounts of data could be conveniently analyzed for average grain sizes, size distributions, etc.

A certain random error was associated with the applied measurement technique. Using the digitizing tablet, it was possible to measure widths to the nearest half millimeter. At the print magnifications employed, this uncertainty corresponded to a $\sim\pm35$ Å uncertainty in the grain size measurement.

IV. RESULTS

Measured grain growth versus ion dose curves are shown in Figs. 1–5. Results are presented for doses up to 3×10^{15} cm^{-2}, which was the largest dose attained for all the samples. At higher doses, in some samples, the films tore or curled, precluding further observation of the microstructure. The solid and dashed lines in Figs. 1–5 are least squared error curve fits for the multilayer and coevaporated data, respectively. The fits were determined according to the expression

$$L^n - L_0^n = K\Phi, \tag{1}$$

where L is the average linear grain size, Φ is the ion dose, L_0 is the best-fit initial grain size, n is the best-fit growth exponent, and K is a best-fit constant. In order to avoid curve fits that yielded negative grain sizes at low doses, it was necessary to treat L_0 as a best-fit variable rather than use the experimentally measured value. The resulting parameters for the fits are given in Table II. Equation (1) is of the form commonly used to describe the kinetics of thermally induced grain growth with Φ replacing time, t. At a constant dose rate, Φ and t are interchangeable.

Irradiation-induced grain growth in the films was observed to be uniform at all the doses examined. No secondary or anomalous grain growth was observed. Figure 6 shows the evolution of the grain size distribution as a function of dose in a Pt-Ti multilayer sample. The distributions were observed to be log-normal, and thus similar to those

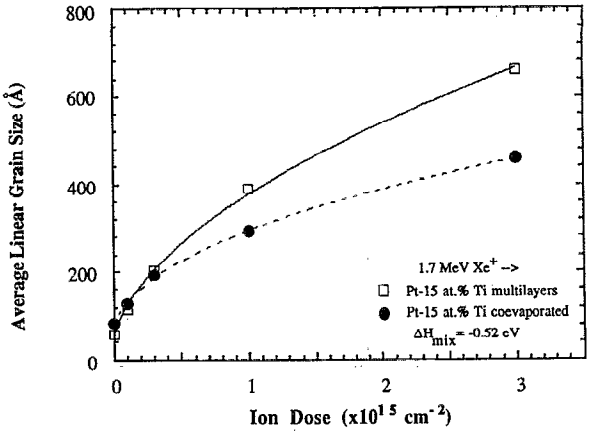

FIG. 1. The effect of ion dose on grain size in Pt-Ti multilayer and coevaporated alloy films ($\Delta H_{mix} = -0.52$ eV). Films were ~400 Å thick and were irradiated with 1.7-MeV Xe ions at room temperature in the HVEM. Solid and dashed lines are best-fit curves to the measured data for the multilayers and coevaporated films, respectively, according to Eq. (1).

observed in thermally induced normal grain growth. The solid lines shown in the figure correspond to best-fit normal distributions to the log-grain-size data.

It was evident that in all the cases except the Pt-Ni and Pt-V films, the multilayers and coevaporated films of the same alloy experienced different grain growth rates and, hence, different final grain sizes after the same dose. An example of this is illustrated by the dark field images of the microstructures shown in Fig. 7. In Figs. 7(a) and 7(b) multilayer and coevaporated Ni-Al films are shown irradiated to the same dose. Similarly, in Figs. 7(c) and 7(d), Pt-Ni coevaporated and multilayer films are shown, respectively, after the same dose. A considerable difference in grain size was observed in the Ni-Al alloy films while considerably less difference was seen in the Pt-Ni films.

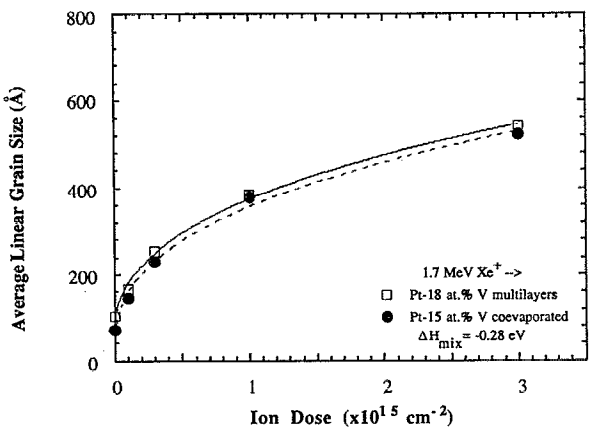

FIG. 2. The effect of ion dose on grain size in Pt-V multilayer and coevaporated alloy films ($\Delta H_{mix} = -0.28$ eV). Films were ~400 Å thick and were irradiated with 1.7-MeV Xe ions at room temperature in the HVEM. Solid and dashed lines are best-fit curves to the measured data for the multilayers and coevaporated films, respectively, according to Eq. (1).

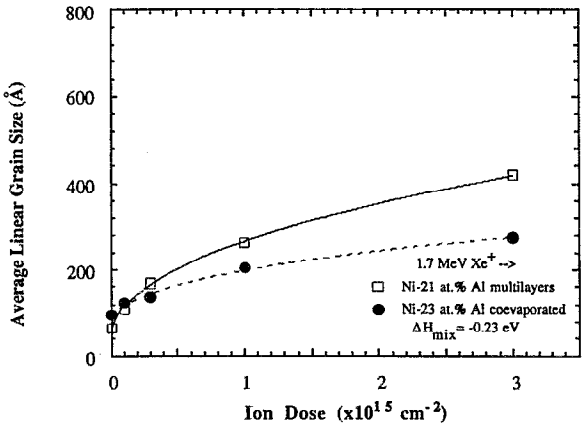

FIG. 3. The effect of ion dose on grain size in Ni-Al multilayer and coevaporated alloy films ($\Delta H_{mix} = -0.23$ eV). Films were ~400 Å thick and were irradiated with 1.7-MeV Xe ions at room temperature in the HVEM. Solid and dashed lines are best-fit curves to the measured data for the multilayers and coevaporated films, respectively, according to Eq. (1).

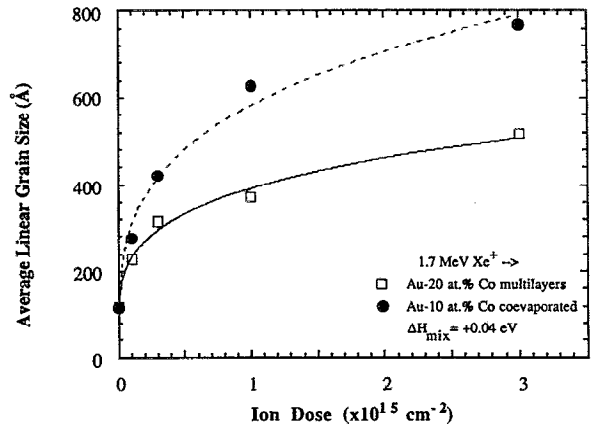

FIG. 5. The effect of ion dose on grain size in Au-Co multilayer and coevaporated alloy films ($\Delta H_{mix} = +0.04$ eV). Films were ~400 Å thick and were irradiated with 1.7-MeV Xe ions at room temperature in the HVEM. Solid and dashed lines are best-fit curves to the measured data for the multilayers and coevaporated films, respectively, according to Eq. (1).

In order to quantify the variations in grain growth, ion-induced grain growth rates, dL/dt, were evaluated. Rates for all the alloys and film types were determined according to $dL/dt = \dot{\Phi} dL/d\Phi$, where $\dot{\Phi}$ was the ion dose rate and $dL/d\Phi$ was obtained from the slopes of the fitted grain growth versus ion dose curves evaluated at a dose of $\Phi = 10^{14}$ cm^{-2} (see Table III). This dose was selected because mixing was expected to be incomplete in the multilayers at this point and in turn the ΔH_{mix} effect would be most pronounced. The incomplete mixing at this dose was confirmed in the Ni-Al samples by electron diffraction observations in which elemental Al ring reflections were observed for doses less than 10^{15} cm^{-2}.

All coevaporated films, with the exception of Ni-Al, were initially formed as extended solid solutions and remained so during irradiation. Again, with the exception of Ni-Al, the multilayer films were homogenized, eliminating the elemental films and forming single phase solid solutions. Diffraction detected no second phases or oxides in any of the films at intermediate doses during irradiation. All the solid solutions were fcc in structure with lattice parameters similar to those of the A alloying element (Pt, Ni, or Au). The Ni-Al alloy films showed formation of the solid solution γ phase and the structurally similar hexagonal close packed (hcp) phase, as observed in previous irradiation-induced phase formation studies.[37]

Irradiation-induced texture was observed in some of the Pt and Au alloys. The texture formed in the solid solutions with the close packed (111) planes of the fcc phase parallel to the film surface. No correlation was observed between the presence (or absence) of this texture and differences in grain growth observed between multilayer and coevaporated films.

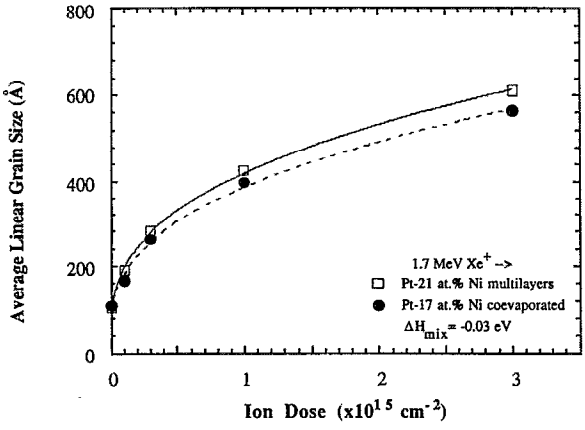

FIG. 4. The effect of ion dose on grain size in Pt-Ni multilayer and coevaporated alloy films ($\Delta H_{mix} = -0.03$ eV). Films were ~400 Å thick and were irradiated with 1.7-MeV Xe ions at room temperature in the HVEM. Solid and dashed lines are best-fit curves to the measured data for the multilayers and coevaporated films, respectively, according to Eq. (1).

TABLE II. Least-squared error curve fit parameters determined for Xe ion-induced grain growth data. Average grain size data, L, and ion dose, Φ, were fit in the dose range from 0 to 3×10^{15} cm^{-2} to the expression: $L = (K\Phi + L_0^n)^{1/n}$.

A-B alloy	Film type[a]	L_0 (Å)	Fit parameters (n)	K (Å^n cm^2)
Pt-Ti	ML	55	1.9	8.60×10^{-11}
	CO	84	2.4	1.00×10^{-9}
Pt-V	ML	102	2.9	2.43×10^{-8}
	CO	68	2.8	1.14×10^{-8}
Pt-Ni	ML	103	2.9	3.25×10^{-8}
	CO	105	2.8	1.76×10^{-8}
Au-Co	ML	119	4.3	1.38×10^{-4}
	CO	114	3.6	8.59×10^{-6}
Ni-Al	ML	65	2.4	6.69×10^{-10}
	CO	98	3.1	1.41×10^{-8}

[a]Film type: ML = multilayers; CO = coevaporated.

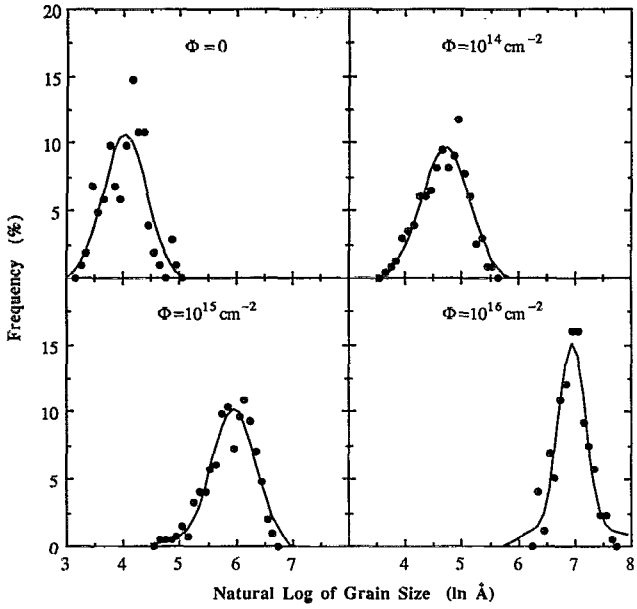

FIG. 6. Evolution of the grain size distribution as a function of ion dose in Pt-15 at. % Ti multilayer alloy films irradiated with 1.7 MeV Xe in the HVEM. Solid lines are normal distributions fit to the measured log grain size data.

V. DISCUSSION

A. Variation in grain growth rates: Multilayers vs coevaporated films

A clear effect of the heat-of-mixing was found in comparing ion-induced grain growth results in multilayer and coevaporated films of the *same* alloy. For a given alloy, both film types were expected to behave in a collisionally similar fashion (same F_D and E_d) and being the same composition, no effect due to alloying was expected (same ΔH_{coh}). Differences in grain growth rates between the two film types were observed to correlate in each alloy with the sign of ΔH_{mix}.

TABLE III. 1.7 MeV Xe ion-induced grain growth rates for multilayer (ML) and coevaporated (CO) alloy films at a dose of $\Phi = 10^{14}$ cm^{-2}.

Alloy	ΔH_{mix}(eV)	$\left.\frac{dL}{dt}\right\|_{ML}\left(\frac{Å}{s}\right)$	$\left.\frac{dL}{dt}\right\|_{CO}\left(\frac{Å}{s}\right)$	$\frac{dL/dt_{ML}}{dL/dt_{CO}}$
Pt-Ti	−0.52	0.95	0.70	1.36
Pt-V	−0.28	0.80	0.82	0.97
Ni-Al	−0.23	0.61	0.32	1.89
Pt-Ni	−0.03	0.91	0.89	1.02
Au-Co	0.04	0.86	1.40	0.61

Multilayers with negative heat-of-mixing ($\Delta H_{mix} < 0$) values showed an enhancement in grain growth rates relative to the coevaporated films, while the opposite was observed for the positive heat-of-mixing ($\Delta H_{mix} > 0$) values. In the Pt-Ti and Ni-Al systems, with their large negative ΔH_{mix} (see Table I), the multilayers experienced faster grain growth than their coevaporated counterparts. In the Pt-Ni system, with a small negative ΔH_{mix}, virtually no difference was observed between multilayers and coevaporated films. The Au-Co system, with a positive ΔH_{mix}, showed results opposite those observed for the large negative ΔH_{mix} systems. In this case, the coevaporated alloy film experienced faster grain growth than the multilayers. The heat-of-mixing correlation is illustrated graphically in Fig. 8.

The exception to the above trend was the Pt-V alloy system, in which both multilayers and coevaporated films experienced nearly identical ion-induced grain growth (see Fig. 2). This occurred despite the fact that the calculated ΔH_{mix} for this system is negative and of the same magnitude as that of Ni-Al (see Table I). It is also observed (Fig. 8) that the Ni-Al alloy showed a substantially larger ratio of multilayer to coevaporated grain growth rates relative to its calculated ΔH_{mix}. Instead, the Pt-Ti system,

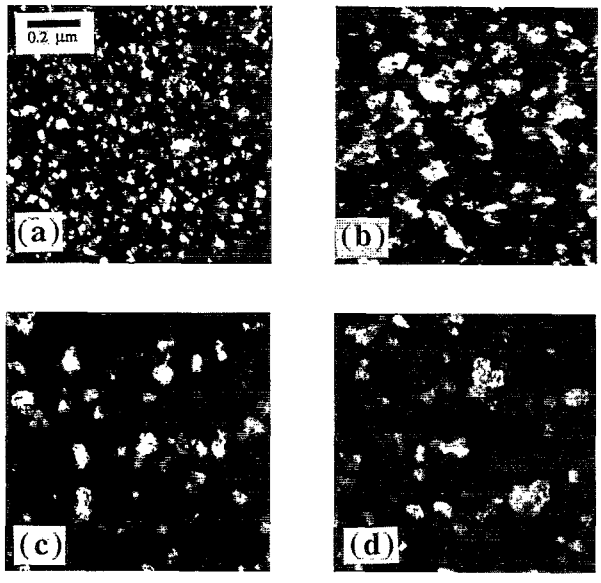

FIG. 7. Comparison of dark field imaged microstructures in multilayer and coevaporated alloy films irradiated with 1.7 MeV Xe–5×10^{15} cm^{-2}. (a) Ni-Al coevaporated, (b) Ni-Al multilayers, (c) Pt-Ni coevaporated, (d) Pt-Ni multilayers.

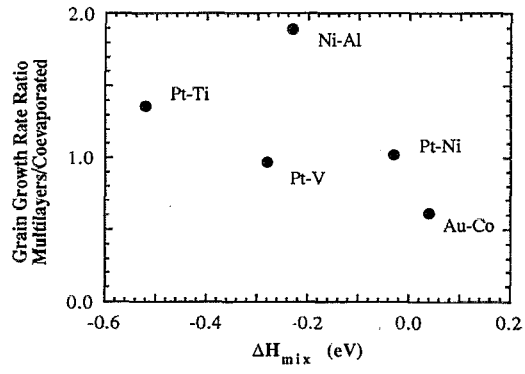

FIG. 8. Variation in instantaneous ion-induced grain growth rate ratios with the heat-of-mixing, ΔH_{mix}. Ratio is the growth rate in multilayer vs coevaporated films evaluated at a dose of $\Phi = 10^{14}$ cm^{-2}.

with the largest calculated negative ΔH_{mix} might be expected to yield the largest ratio. The deviations represented by both the Pt-V and Ni-Al systems are likely due in large part to uncertainty in the actual ΔH_{mix} values for the irradiated multilayer systems. The uncertainty associated with approximating ΔH_{mix} with ΔH_{for}, as discussed in the experimental section, is expected to contribute to the disparities observed in the data. The deviations in these two alloy systems may also be indicative that the heat-of-mixing effect may not be solely responsible for the variation in grain growth rates among the ML and CO film types.

After a sufficient ion dose, mixing of the multilayers will be complete, and it is to be expected that the ΔH_{mix} effect will disappear, yielding no grain growth rate differences between ML and CO films of the same alloy. Based on the experimental results represented in Figs. 1–5 it is not possible to confirm such a disappearance in these experiments. No measurements were made of the dose dependence of intermixing, and therefore it is not possible to comment absolutely on the degree of intermixing achieved in the multilayers after the largest dose (3×10^{15} cm^{-2}) examined in this work. Likewise, uncertainty in grain size measurements prevents commenting absolutely on differences in grain growth rates that may exist between ML and CO films at the large doses. Because of these uncertainties, the grain growth rate analysis was restricted to a low ion dose (10^{14} cm^{-2}), in which mixing was clearly incomplete and in turn where the ΔH_{mix} effect would be most pronounced.

The correlations discussed above suggest that the heat-of-mixing affects the kinetic mechanisms of ion-induced grain growth. The magnitude of ΔH_{mix} in many of the alloys, as shown in Table I, is quite substantial in comparison with activation energies for ion-induced grain growth in thin films which are typically on the order of 0.1 eV.[6] One possibility is that as ion beam mixing proceeds in multilayers, a ΔH_{mix} enthalpy release or absorption (depending on the sign of ΔH_{mix}) occurs that thermally enhances or inhibits atomic migration and hence grain boundary migration. Another possibility is an affect on grain growth via a Darken effect,[26] in which atomic mobility across grain boundaries, located in the concentration gradients of the multilayers, is either enhanced or inhibited according to the sign of the heat-of-mixing. In either case, it is clear that ΔH_{mix} significantly impacts grain growth kinetics in the multilayers.

B. Variations in grain growth rates among coevaporated films

The differences observed in growth rates among the collisionally similar films used in this study indicated that a purely collisional (displacement rate) approach was inadequate for describing ion-induced grain growth in coevaporated films. As indicated in Table I, all the alloys used in the irradiations, except Ni-Al, experienced nearly the same deposited damage energy, F_D. However, considerable differences were observed in ion-induced grain growth rates. From Table III Au-Co coevaporated films were observed to have a factor of two greater grain growth rate than Pt-Ti coevaporated films. According to TRIM-90 calculations, both of these alloys have nearly identical F_D values and since they also have similar E_d values, both are expected to undergo essentially identical displacement damage.

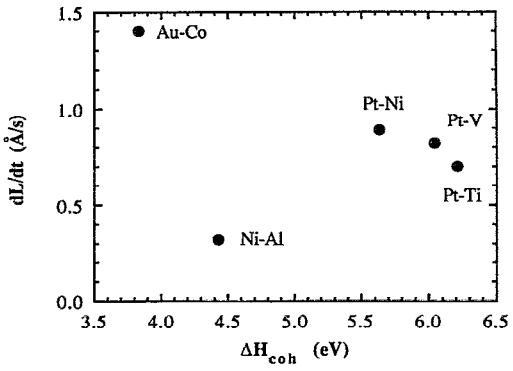

FIG. 9. Variation in instantaneous ion-induced grain growth rate in coevaporated alloys with the alloy cohesive energy, ΔH_{coh}. Rates evaluated at a dose of $\Phi = 10^{14}$ cm^{-2}.

The conclusion that collisional displacements alone are inadequate for describing ion-induced grain growth is consistent with previous observations of Liu *et al.*[13] and Li *et al.*[5] Their results and those of the present study demonstrate that an understanding of the ion-induced grain growth process also requires consideration of material-related properties such as the effects of alloying (in multilayers and coevaporated films) and the heat-of-mixing (in multilayers).

Differences in growth rates found in the present study among the coevaporated films are clearly related to differences in material-related properties of the films. Alloying could substantially modify film properties, such as the activation energy for grain growth, and in turn, enhance or inhibit grain growth. Figure 9 shows the variation in grain growth rate of irradiated coevaporated films plotted against the average cohesive energy, ΔH_{coh}, of the alloy. With the exception of Ni-Al, alloys with low average cohesive energy underwent faster grain growth. The low grain growth rate observed for the Ni-Al system might have been due to the inhibiting effect of a second phase in the film. The HCP phase forms during irradiation in this system, and its presence could inhibit the migration of grain boundaries.[38]

Comparison of ion-induced grain growth rates among only the multilayer alloy films fails to show a simple qualitative correlation with the heat-of-mixing or the cohesive energy, as demonstrated in Table III. In fact the grain growth rates appear to scale with F_D. However, such an observation is tempered by the fact that second phase particle inhibition may have affected the grain growth rate in the Ni-Al multilayers, complicating a direct in terms of F_D interpretation. Furthermore, the fit parameters in Table II and resulting curve fits in Figs. 1–5 suggest substantially different grain growth kinetics among the multilayers. Therefore the similarity of grain growth rates (with the

exception of Ni-Al) at the single dose examined may simply be fortuitous.

The observations associated with ion-induced grain growth described above were in many ways analogous to those associated with ion beam mixing, suggesting that both phenomena are governed by the same irradiation-induced effects. Systematic studies of ion beam mixing were performed by Cheng *et al.*,[39] Van Rossum *et al.*[40] and Johnson *et al.*[27] examining bilayer intermixing under heavy ion irradiation. Their results showed that the rate of intermixing varied considerably among alloys with similar F_D. Also ΔH_{mix} was observed to affect the intermixing rate, with large negative ΔH_{mix} promoting faster intermixing. The magnitudes of intermixing rates were considerably greater than what was predicted from pure collisional irradiation considerations.

C. Variation in growth exponents

The kinetics of grain growth are often characterized by the growth exponent n [see Eq. (1)] under specific experimental conditions (e.g., anneal temperature, sample purity, etc.).[24] Normal grain growth, which is driven by the reduction in total surface energy, ideally follows parabolic, $n=2$, kinetics. In thermal annealing experiments, a number of factors have been identified that inhibit grain growth, yielding nonparabolic ($n>2$) kinetics. These same factors can be expected to operate in ion-induced grain growth. Impurity atoms, porosity, gas bubbles, free surfaces, and second phase particles are believed to inhibit boundary migration via a drag mechanism. As a result of the inhibition, parabolic kinetics are prevented yielding $n>2$.[39]

In this study, growth exponents determined from fits to the grain size data (see Table II), varied from a low value of $n=1.9$ for Pt-Ti multilayers to a high value of $n=4.3$ for Au-Co multilayers. The average lies in the vicinity of $n=3.0$, similar to the values determined by Atwater *et al.*[3] and Liu *et al.*[6] for irradiated elemental films. The variations in growth exponents observed in this study were clearly larger than any deviations attributable to experimental uncertainty. Through a simple parametric analysis it was estimated that the uncertainty in individual grain size measurement (± 35 Å) accounted for an $\sim 10\%$ variation in growth exponent values determined from curve fits.

It is uncertain from this study or previous studies as to the precise origin of the nonparabolic ($n>2$) kinetics observed in ion-induced grain growth. Assuming ion-induced grain growth proceeds similar to thermal grain growth (continuous boundary migration driven by boundary curvature), it is possible to argue that nonparabolic kinetics arise from the presence of inhibiting driving forces as mentioned above. However, the nonparabolic kinetics may instead indicate that ion-induced grain growth proceeds by a kinetic mechanism fundamentally different from that of thermal normal grain growth.

VI. CONCLUSIONS

In situ grain growth studies on coevaporated and multilayer films were conducted on *A*-rich, *A-B* (Pt-Ti, Ni-Al, Pt-V, Pt-Ni, and Au-Co) alloy films irradiated at room temperature with 1.7-MeV Xe ions. The findings supported the following conclusions.

The initial structure of the films, multilayered versus coevaporated, was observed to significantly affect subsequent ion-induced grain growth. Within each particular alloy, in all but one case (Pt-V), the ion-induced grain growth rate in multilayer films was greater than the rate in coevaporated films for $\Delta H_{\text{mix}} < 0$ and the coevaporated rate was greater than the multilayer rate for $\Delta H_{\text{mix}} > 0$. However, the multilayer grain growth rates did not vary with the calculated magnitude of ΔH_{mix} between alloy systems. Variations in grain growth rates among collisionally similar coevaporated alloys suggested that a purely collisional approach was inadequate for describing ion-induced grain growth.

In all the films, normal grain growth was induced by irradiation with the average grain size increasing with ion dose according to $L^n - L_0^n = K\Phi$. Deviations ($n=1.9$–4.3) from ideal parabolic ($n=2$) grain growth kinetics for the data of this study were possibly due to the effect of inhibiting driving forces.

ACKNOWLEDGMENTS

The authors gratefully acknowledge the use of facilities and assistance provided by the following: High Voltage Electron Microscope-Tandem Facility (L. Funk, S. Ockers, and E. Ryan) at ANL, Michigan Ion Beam Laboratory for Surface Modification and Analysis (A. Mashayekhi and V. Rotberg) and Electron Microscopy and Analysis Laboratory (J. Mansfield) both at the University of Michigan. Thanks are also extended to H. Atwater for grain size measurement software and C. Allen and J. Liu for helpful discussions. This work was funded under NSF Grants No. DMR8603174 and No. DMR8903138 (D. Alexander and G. Was) and DOE Contract No. W-31-109-ENG-38 (L. Rehn).

[1] P. Wang, D. A. Thompson, and W. W. Smeltzer, Nucl. Instrum. Methods B **16**, 288 (1986).

[2] P. Wang, D. A. Thompson, and W. W. Smeltzer, Nucl. Instrum. Methods B **7/8**, 97 (1985).

[3] H. A. Atwater, C. V. Thompson, and H. I. Smith, Phys. Rev. Lett. **60**, 112 (1988).

[4] H. A. Atwater, C. V. Thompson, and H. I. Smith, in *Fundamentals of Beam-Solid Interactions and Transient Thermal Processing*, edited by M. J. Aziz, L. E. Rehn, and B. Strizker (Materials Research Society, Pittsburgh, PA, 1988), pp. 345–356.

[5] J. Li, J. C. Liu, and J. W. Mayer, Nucl. Instrum. Methods B **36**, 306 (1989).

[6] J. C. Liu, J. Li, and J. W. Mayer, J. Appl. Phys. **67**, 2354 (1990).

[7] J. C. Liu and J. W. Mayer, Nucl. Instrum. Methods B **19/20**, 538 (1987).

[8] J. C. Liu, M. Nastasi, and J. W. Mayer, J. Appl. Phys. **62**, 423 (1987).

[9] J. C. Liu, J. Li, J. W. Mayer, C. W. Allen, and L. E. Rehn, in *Processing and Characterization of Materials Using Ion Beams*, edited by L. E. Rehn, J. Green, and F. A. Smidt (Materials Research Society, Pittsburgh, PA, 1989), pp. 297–302.

[10] J. C. Liu and J. W. Mayer, in *Fundamentals of Beam-Solid Interactions*

and Transient Thermal Processing, edited by M. J. Aziz, L. E. Rehn, and B. Strizker (Materials Research Society, Pittsburgh, PA, 1988), pp. 357–362.
[11] C. W. Allen and L. E. Rehn, in *Beam Solid Interactions: Physical Phenomena,* edited by J. A. Knapp, P. Borgesen, and R. A. Zuhr (Materials Research Society, Pittsburgh, PA, 1990), pp. 99–104.
[12] C. W. Allen, in *Proceedings of the Forty-Seventh Annual Meeting of the Electron Microscopy Society of America,* edited by G. W. Bailey (San Francisco Press, Inc., San Francisco, CA, 1989), pp. 644–645.
[13] J. C. Liu, thesis, Cornell University, Ithaca, NY, 1989.
[14] B. Y. Tsaur, S. S. Lau, L. S. Hung, and J. W. Mayer, Nucl. Instrum. Methods **182/183**, 67 (1981).
[15] J. M. Eridon, G. S. Was, and L. E. Rehn, J. Appl. Phys. **62**, 2145 (1987).
[16] B. Y. Tsaur, S. S. Lau, and J. W. Mayer, Appl. Phys. Lett. **36**, 823 (1980).
[17] B. Y. Tsaur and M. Maenpaa, J. Appl. Phys. **52**, 728 (1981).
[18] D. E. Alexander, G. S. Was, and J. M. Eridon, Nucl. Instrum. Methods B **39**, 130 (1989).
[19] R. J. Gaboriaud, J. J. Grob, and F. Abel, Nucl. Instrum. Methods B **19**, 648(1987).
[20] U. G. Akano, D. A. Thompson, W. W. Smeltzer, and J. A. Davies, J. Mater. Res **3**, 1063 (1988).
[21] A. M. Ibrahim and D. A. Thompson, Nucl. Instrum. Methods B **7/8**, 566 (1985).
[22] D. E. Alexander, G. S. Was, and L. E. Rehn, in *Beam Solid Interactions: Physical Phenomena,* edited by J. A. Knapp, P. Borgesen, and R. A. Zuhr (Materials Research Society, Pittsburgh, PA, 1990), pp. 155–160.
[23] S. K. Prasad, H. Herman, A. H. King, and A. Goland, in *Proceedings Electron Microscopy Society of America,* edited by G. W. Bailey (Claitor's Publishing Division, Baton Rouge, LA, 1982), p. 634.
[24] H. V. Atkinson, Acta Metall. **36**, 469 (1988).
[25] C. V. Thompson, J. Appl. Phys. **58**, 763 (1985).
[26] P. S. Shewmon, *Diffusion in Solids* (The Minerals, Metals, & Materials Society, Warrendale, PA, 1989).
[27] W. L. Johnson, Y. T. Cheng, M. Van Rossum, and M-A. Nicolet, Nucl. Instrum. Methods B **7/8**, 657 (1985).
[28] C. Kittel, *Introduction to Solid State Physics,* 5th ed. (Wiley, New York, 1976), p. 74.
[29] A. K. Niessen, A. R. Miedema, F. R. De Boer, and R. Boom, Physica B **152**, 303 (1988).
[30] A. K. Niessen, A. R. Miedema, F. R. De Boer, and R. Boom, Physica B **151**, 401 (1988).
[31] F. R. De Boer, R. Boom, and A. R. Miedema, Physica **101B**, 294 (1980).
[32] J. P. Biersack and L. G. Haggmark, Nucl. Instrum. Methods **174**, 257 (1980).
[33] A. R. Miedema, P. F. de Chatel, and F. R. de Boer, Physica **100B**, 1 (1980).
[34] B. X. Liu, W. L. Johnson, and M-A. Nicolet, Nucl. Instrum. Methods **209/210**, 229 (1983).
[35] M. Hansen and K. Anderko, *Constitution of Binary Alloys,* 2nd ed. (McGraw-Hill, New York, 1958).
[36] C. W. Allen, L. L. Funk, E. A. Ryan, and A. Taylor, Nucl. Instrum. Methods B **40/41**, 553 (1989).
[37] D. E. Alexander, G. S. Was, and L. E. Rehn, J. Appl. Phys. **69**, 2021 (1991).
[38] E. A. Grey and G. T. Higgins, Acta Metall. **21**, 309 (1973).
[39] Y. T. Cheng, M. Van Rossum, M-A. Nicolet, and W. L. Johnson, Appl. Phys. Lett. **45**, 185 (1984).
[40] M. Van Rossum, Y. T. Cheng, M-A. Nicolet, and W. L. Johnson, Appl. Phys. Lett. **46**, 610 (1985).